Learning from Demonstration and Adaptation of Biped Locomotion with Dynamical Movement Primitives

Jun Nakanishi*[1], Jun Morimoto[1], Gen Endo[1,2], Gordon Cheng[1], Stefan Schaal[1,3] and Mitsuo Kawato[1]

[1]ATR Computational Neuroscience Laboratories, Kyoto 619–0288, Japan
[2]Sony Intelligent Dynamics Laboratory, Tokyo 141–0001, Japan
[3]University of Southern California, Los Angeles, CA 90089-2520, USA

***Abstract*— In this paper, we report on our research for learning biped locomotion from human demonstration. Our ultimate goal is to establish a design principle of a controller in order to achieve natural human-like locomotion. We suggest dynamical movement primitives as a CPG of a biped robot, an approach we have previously proposed for learning and encoding complex human movements. Demonstrated trajectories are learned through the movement primitives by locally weighted regression, and the frequency of the learned trajectories is adjusted automatically by a novel frequency adaptation algorithm based on phase resetting and entrainment of oscillators. Numerical simulations demonstrate the effectiveness of the proposed locomotion controller.**

I. INTRODUCTION

There has been a growing interest in biped locomotion with the recent development of humanoid robots. Many of existing successful walking algorithms use the zero moment point (ZMP) criterion [21] for motion generation with off-line planning [9], [20] and on-line balance compensation [5], [8], [23]. These ZMP methods have been shown to be effective to guarantee point-wise stability of biped locomotion. However, they require precise modelling of robot dynamics and high-gain trajectory tracking control, and the generated patterns result in a typical "bent-knee" posture to avoid singularities. From the viewpoint of energy efficiency, such walking patterns are not desirable since torque must be continuously applied to the knee joint to maintain a bent-knee posture. The previous ZMP approaches have primarily focused on stability during walking rather than natural human-like motion which exploits passive dynamics of the body.

In contrast to off-line trajectory planning, biologically-inspired control approaches based on central pattern generators (CPGs)[1] with neural oscillators have been drawing much attention for rhythmic motion generation. As a CPG, a neural oscillator proposed by Matsuoka [12] is widely used, which models the firing rate of two mutually inhibiting neurons described in a set of differential equations. This model is used in robotic applications to achieve designated tasks involving rhythmic motion which requires interactions between the system and the environment. Examples include biped locomotion [4], [19], quadruped locomotion [3], juggling [13], drumming [11], and playing with a slinky toy [22]. Neural oscillators have desirable properties such as adaptation to the environment through entrainment. However, it is difficult to design robust controllers with coupled oscillators, and to manually tune all open parameters to achieve a desired behavior.

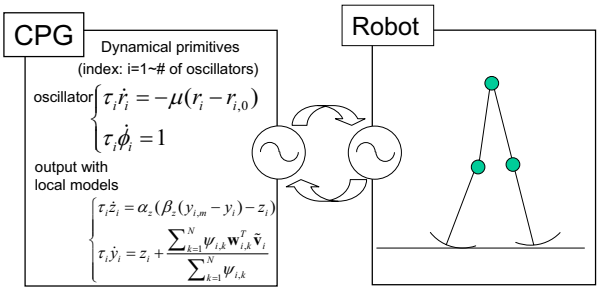

Fig. 1. Proposed control strategy: CPG with dynamical movement primitives and the robot.

In this paper, we suggest an approach to learning biped locomotion from human demonstration and its adaptation through coupling between the pattern generator and the mechanical system. Motivated by human's capability of learning and imitating a demonstrated movement by others, imitation learning has been explored as an efficient method for motor learning in robots to accomplish the desired movement [16], [17]. Previously, Ijspeert, Nakanishi and Schaal have proposed a method to encode complex discrete and rhythmic multijoint movements through imitation learning as movement primitives [6], [7]. Kinematic movement plans are described in a set of nonlinear differential equations with well-defined attractor dynamics, and demonstrated trajectories are learned using

*Email: jun@atr.co.jp

[1]The term CPG is widely used, but a distributed pattern generator (DPG) may be more appropriate, since, in many robotic applications, a distributed architecture which consists of coupled oscillators is generally used for pattern generators. In this paper, we shall use the classic term CPG although we consider much more a DPG-like distributed architecture.

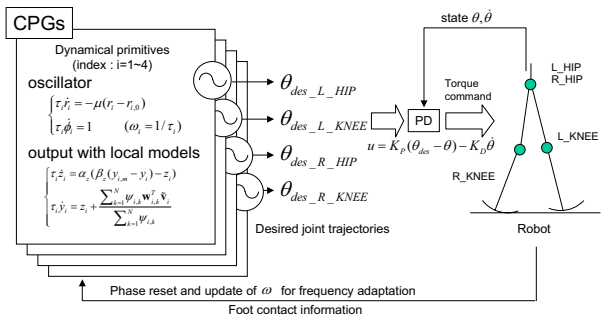

Fig. 2. Robot controller with dynamical movement primitives.

locally weighted regression. In this paper, we present the idea of using rhythmic movement primitives [7] as a CPG to achieve natural human-like walking in biped robots. Figure 1 depicts a conceptual architecture of the proposed control system. The dynamical movement primitive [7] has various desirable properties which are beneficial for biped locomotion—for example, it can learn a demonstrated trajectory rapidly, and it is easy to re-scale the learned rhythmic movement in terms of amplitude, frequency and offset of the patterns. In this work, we also propose an adaptation algorithm for the frequency of walking based on phase resetting [10] and entrainment between the phase oscillator and mechanical system using feedback from the environment. We present numerical simulations to demonstrate the effectiveness of the proposed control strategy.

II. Learning Biped Locomotion from Human Demonstration

A. Rhythmic Dynamical Movement Primitives

We briefly review the rhythmic dynamical movement primitives proposed in [7], which we will use as a CPG for biped locomotion in this paper. Consider the following limit cycle oscillator characterized in terms of an amplitude r and a phase ϕ as a canonical dynamical system which generates basic rhythmic patterns:

$$\tau\dot{\phi} = 1 \tag{1}$$

$$\tau\dot{r} = -\mu(r - r_0) \tag{2}$$

where τ is a temporal scaling factor, r_0 determines the desired (relative) amplitude, and μ is a positive constant. Note that the phase dynamics (1) can be written as

$$\dot{\phi} = \omega \tag{3}$$

where $\omega \stackrel{\text{def}}{=} 1/\tau$ is the natural frequency. This rhythmic canonical system is designed to provide an amplitude signal $\tilde{\mathbf{v}} = [r\cos\phi, r\sin\phi]^T$ and phase variable $\mathrm{mod}(\phi, 2\pi)$ to the the following second order dynamical system (z, y), where the output y is used as the desired trajectory for the robot.

$$\tau\dot{z} = \alpha_z(\beta_z(y_m - y) - z) \tag{4}$$

$$\tau\dot{y} = z + f(\tilde{\mathbf{v}}, \phi) \tag{5}$$

where α and β are time constants, y_m is an offset of the output trajectory. f is a nonlinear function approximator using locally linear models [15] of the form

$$f(\tilde{\mathbf{v}}, \phi) = \frac{\sum_{k=1}^{N} \Psi_k \mathbf{w}_k^T \tilde{\mathbf{v}}}{\sum_{i=k}^{N} \Psi_k}. \tag{6}$$

where $\mathbf{w}_k$ is the parameter vector of the k-th local model which will be determined by locally weighted learning [15] from a demonstrated trajectory y_{demo} (see Section II-C.2). Each local model is weighted by a Gaussian kernel function

$$\Psi_k = \exp(-h_k(\mathrm{mod}(\phi, 2\pi) - c_k)^2) \tag{7}$$

where c_k is the center of the k-th linear model, and h_k characterizes its width. A final prediction is calculated by the weighted average of the predictions of the individual models. As demonstrated in [7], the amplitude, frequency and offset of the learned rhythmic patterns can be easily modified by scaling the parameters r_0, $\omega(= 1/\tau)$ and y_m individually.

B. Rhythmic Dynamical Movement Primitives as a CPG

We use the rhythmic dynamical movement primitives introduced above as a CPG. Figure 2 illustrates the proposed control architecture in this paper. Each joint is equipped with a movement primitive which generates the desired joint trajectory θ_{des}. We define the index and the corresponding name of the joint as Left hip (i=1, L_HIP), and Left knee (i=2, L_KNEE), Right hip (i=3, R_HIP), and Right knee (i=4, R_KNEE). In this setting, each degree of freedom (DOF) has its own oscillator, however, different allocation of oscillators can be considered, e.g., a unique oscillator for the whole CPG or one oscillator for each leg. We will address this design issue in our future work. A low-gain PD controller is used for each joint to track the desired trajectory which is the output of the movement primitive, and ground contact information is fed back to the CPG in order to reset the phase and adjust the natural frequency of the oscillators. At heel contact, the phase of all the oscillators is reset to $\phi = 0$ for the stance leg and to $\phi = \pi$ for the swing leg respectively at the same time. Thus, the phase difference between the oscillators for the left leg and the right leg is kept π rad. The update law for the frequency adaptation of locomotion will be discussed in Section III-B in detail.

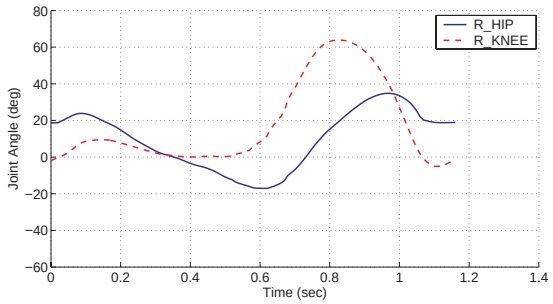

Fig. 3. Extracted one period of joint trajectory data of human walking presented in [2] as used for learning in this paper (R_HIP and R_KNEE).

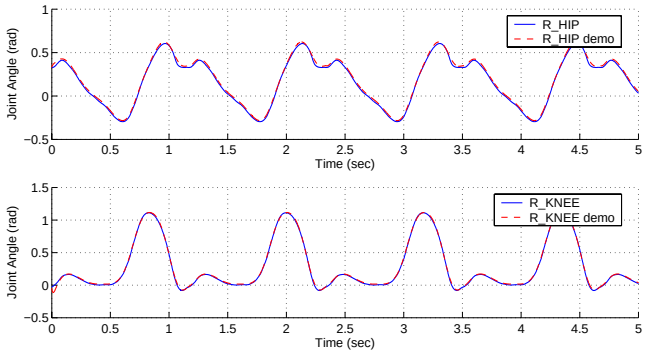

Fig. 4. Learning result of human's walking trajectories using dynamical movement primitives. The learned trajectories (output of the dynamical primitives) nearly coincide the demonstrated trajectories.

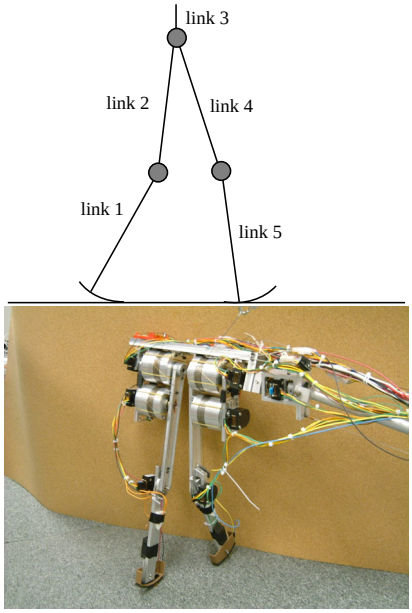

Fig. 5. Top: Five-link model of the robot. Bottom: physical system whose dynamics are simulated in the numerical studies.

TABLE I

PHYSICAL PARAMETERS OF THE ROBOT MODEL

	link1	link2	link3	link4	link5
mass [kg]	0.05	0.43	1.0	0.43	0.05
length [m]	0.2	0.2	0.01	0.2	0.2
inertia ($\times 10^{-4}$ [kg·m])	1.75	4.29	4.33	4.29	1.75

C. Learning from Human Demonstration

1) Human's Walking Pattern: As a demonstrated trajectory, we use the recorded joint data of human walking in the book [2] (29-year-old male, 173cm, 83.5kg, right hip and knee). In the future, we plan to measure human walking under various conditions by ourselves using our motion capture equipment. Figure 3 shows the extracted trajectory data of the right hip and knee joints for one period of locomotion from [2]. In the next section, we will use these joint trajectories as human demonstration for the learning of biped locomotion. We identified the period and frequency of this patten by the power spectrum estimation with FFT and autocorrelation as $T = 1.17$ sec and $f = 1/T = 0.855$ Hz respectively.

2) Learning with Locally Weighted Regression: We briefly explain how we find the parameters $\mathbf{w}_k$ in (6) by locally weighted learning [15] for a given demonstrated trajectory y_{demo}. Given a sampled data point $(f_{target}, \tilde{\mathbf{v}})$ at t where

$$f_{target} = \dot{y}_{demo} - \beta(y_m - y_{demo}) \tag{8}$$

the learning problem is formulated to find the parameters $\mathbf{w}_k$ in (6) using incremental locally weighted regression technique [15] in which $\mathbf{w}_i$ is updated by

$$\mathbf{w}_k^{t+1} = \mathbf{w}_k^t + \mathbf{P}_k^{t+1}\tilde{\mathbf{v}}e_k \tag{9}$$

where

$$\mathbf{P}_k^{t+1} = \frac{1}{\lambda}\left(\mathbf{P}_k^t - \frac{\mathbf{P}_k^t\tilde{\mathbf{v}}\tilde{\mathbf{v}}^T\mathbf{P}_k^t}{\frac{\lambda}{\Psi_k} + \tilde{\mathbf{v}}^T\mathbf{P}_k^t\tilde{\mathbf{v}}}\right),\ e_k = f_{target} - \mathbf{w}_k^T\tilde{\mathbf{v}}$$

and $\lambda \in [0,1]$ is a forgetting factor. We chose this locally weighted regression framework as it can automatically find the correct number of necessary basis function, and can tune the h_k parameters of each Gaussian kernel function (7) to achieve higher function approximation accuracy. Moreover, it learns the parameters $\mathbf{w}_k$ of every local model k totally independent of all other local models, which minimizes interference between local models. Figure 4 shows the learning result of the demonstrated trajectories using the rhythmic dynamical primitives. In the book [2], only the trajectory data of the right leg are provided. Thus, we generate the desired trajectory for the left leg by shifting the phase of the oscillator of the right leg by π.

TABLE II

PARAMETERS USED IN THE SIMULATIONS

	Parameter	Description	Value used
Dynamical primitives	r_0	(relative) amplitude	0.7 for all joints
	ω	natural frequency	updated by (19)
	y_m	offset	Hip: $y_m = 0.0$ and Knee: $y_m = 0.35$
PD gains	K_P	position gain	Hip: $K_P = 8.0$ and Knee: $K_P = 6.0$
	K_D	velocity gain	0.05 for all joints
Phase resetting	ϕ_i	phase	$\phi_1 = \phi_2 = 0, \phi_3 = \phi_4 = \pi$ at left leg heel strike
			$\phi_1 = \phi_2 = \pi, \phi_3 = \phi_4 = 0$ at right leg heel strike

III. FREQUENCY ADAPTATION OF LOCOMOTION VIA ENTRAINMENT OF PHASE OSCILLATOR

A. Synchronization of Coupled Phase Oscillators

1) Entrainment with Phase Coupling: This section reviews basic properties of coupled oscillators [18]. Consider the following dynamics of two coupled oscillators as depicted in Figure 6

$$\dot{\phi}_1 = \omega_1 + K_1(\phi_2 - \phi_1) \tag{10}$$
$$\dot{\phi}_2 = \omega_2 + K_2(\phi_1 - \phi_2) \tag{11}$$

where $\omega_1, \omega_2 > 0$ are natural frequencies of the oscillators, and K_1, K_2 are positive coupling constants. Define the phase difference ψ as $\psi = \phi_2 - \phi_1$, and consider its dynamics

$$\dot{\psi} = (\omega_2 - \omega_1) - (K_1 + K_2)\psi. \tag{12}$$

Then, we see that there is a stable fixed point at

$$\psi^* = \frac{\omega_2 - \omega_1}{K_1 + K_2}. \tag{13}$$

As a result, these oscillators run at the same frequency (called coupled frequency) given by

$$\omega^* = \frac{K_2\omega_1 + K_1\omega_2}{K_1 + K_2} \tag{14}$$

with phase difference ψ^*.

2) Synchronization with Frequency Adaptation: In the development above, the oscillators run with the phase difference $\psi = \phi_2 - \phi_1 = \frac{\omega_2 - \omega_1}{K_1 + K_2}$ given ω_1 and ω_2 when they are entrained. Suppose $\omega_1 = \omega_2$, then the phase difference of these oscillators will be zero. Thus, when $\omega_2 = const.$ is given, we introduce a coupling dynamics of the natural frequency for ω_1 in (16) in addition to the phase coupling in order to achieve synchronization of these oscillators with zero phase difference.

$$\dot{\phi}_1(t) = \omega_1(t) + K_1(\phi_2(t) - \phi_1(t)) \tag{15}$$
$$\dot{\omega}_1(t) = -K(\omega_2 - \omega_1(t)) \tag{16}$$
$$\dot{\phi}_2(t) = \omega_2 + K_2(\phi_1(t) - \phi_2(t)) \tag{17}$$

where K is a positive constant. It is straightforward to see that $\omega_1 \to \omega_2$ asymptotically. Thus, the phase difference will be zero as $\psi = \phi_2 - \phi_1 \to 0$.

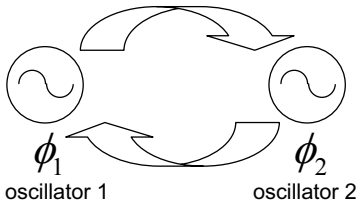

Fig. 6. A coupled phase oscillator system

B. Frequency Adaptation of Locomotion

As depicted in Figure 1, we see that the proposed control system can be regarded as a coupling of the CPG and the mechanical oscillator (robot), which can be modelled analogous to the coupled oscillator system above. Thus, it is natural to introduce such an adaptation mechanism to our dynamical primitives in order to achieve frequency adaptation of the learned periodic motions by the robot itself through the interaction among the CPG, robot and environment.

Consider the following update law of the phase and frequency of the oscillator in the dynamical movement primitives at the instance of heel strike

$$\dot{\phi} = \hat{\omega}^n + \delta(t - t_{heel\ strike})(\phi^{robot}_{heel\ strike} - \phi) \tag{18}$$
$$\hat{\omega}^{n+1} = \hat{\omega}^n + K(\omega^n_{measured} - \hat{\omega}^n) \tag{19}$$

where δ is the Dirac's delta function, n is the number of steps, and $\phi^{robot}_{heel\ strike}$ is the phase of the mechanical oscillator (robot) at heel strike defined as $\phi^{robot}_{heel\ strike} = 0$ at the heel strike of the leg with the corresponding oscillator, and $\phi^{robot}_{heel\ strike} = \pi$ at the heel strike of the other leg. $\omega^n_{measured}$ is the measured frequency of locomotion defined by

$$\omega^n_{measured} = \frac{\pi}{T^n_{measured}} \tag{20}$$

where $T^n_{measured}$ is the time for one step of locomotion (half period with respect to the oscillator). Note that (18) introduces phase resetting to the oscillator at heel strike, and (19) is the discretized version of (16).

IV. Numerical Simulations

In this paper, we present numerical simulations to illustrate the effectiveness of the proposed control algorithm.

A. Robot Model

In the numerical simulations, we use the model of the planar 5-link biped robot [14] depicted in Figure 5. The height of the robot is 40cm and the weight is about 3kg. Kinematic and dynamic parameters of the simulated robot are chosen to match those of the physical system (see Table I). We assume that the motion of the robot is constrained on the sagittal plane. The dynamics of the robot are derived using SD/FAST[2] and integrated using the Runge-Kutta algorithm at 1ms step size. The ground contact force is calculated using a linear spring-damper model.

B. Simulation Results

It is necessary to properly scale the learned trajectories from human demonstration since they cannot be directly applied for the robot model with different dimensions. In the following simulations, the parameters of the dynamical movement primitives and gains of the PD controller are determined empirically as listed in Table II to achieve stable walking. We manually designed the desired trajectory for the initial step from the standing position, and the CPG controller is activated at heel contact of the first step. For the scaling of the natural frequency of the oscillator, the adaptation law proposed in Section III-B is used. Figures 7 and 8 shows the desired and actual joint trajectories[3] for $t = 0 \sim 10$ sec. Figure 9 illustrates the desired and actual joint trajectories, and the timing of heel strke for the left leg. Figure 10 shows the torque command for the left leg, which indicates that the knee joint swings passively since it requires almost no torque (see $t = 14.8 \sim 15.0$ sec).

C. Frequency Adaptation of Locomotion

We present simulation results of the frequency adaptation algorithm proposed in Section III-B. The frequency of the all the oscillators are updated by (18) and (19) at heel contant. Figure 12 (left) depicts the duration for one step and Figure 12 (right) shows the learning curve of the frequency of the CPG with different coupling constants $K = 0.2, 0.5$ and 0.8 in (19) when the initial value is set to $\omega_0 = 4.78$ rad/s (period of oscillation is 1.5 sec). The simulation results demonstrate that robust self-adaptation of the frequency of locomotion is achieved by the proposed algorithm through entrainment. The resultant frequency was $\omega = 8.120$ rad/s. This result may be interpreted as follows: Given the walking frequency of the

[2] `http://www.sdfast.com`

[3] Note that the sign of the trajectories for the hip joints (L_HIP, R_HIP) is opposite to the human demonstration due to the definition of coordinate system.

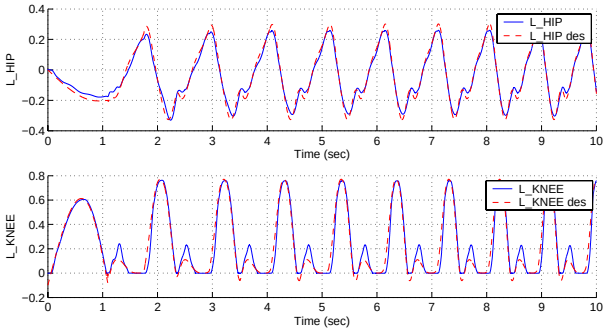

Fig. 7. Joint trajectories of the robot simulation (left leg)

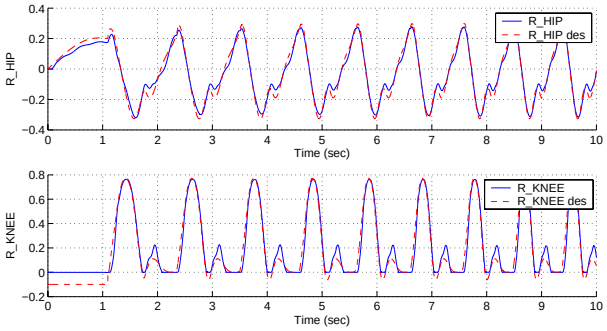

Fig. 8. Joint trajectories of the robot simulation (right leg)

human, ω_{human}, the leg length of the human, l_{human} , and the leg length of the robot, l_{robot}, as depicted in Figure 13, it may be natural to think of the scaling law

$$\hat{\omega}_{robot} = \omega_{human}\sqrt{\frac{l_{robot}}{l_{human}}} \tag{21}$$

which is derived from the ratio of the natural frequency of the simplified linear pendulum. In this paper, l_{human} can be considered as $l_{human} = 1.76 \times 0.49 = 0.86$m since the height of the human subject is 1.76m and it is anatomically known that the leg length is about 49% of the body height [1]. Thus, using the scaling law (21), we can estimate the frequency of locomotion of the robot with $l_{robot} = 0.4$m as

- Frequency: $\hat{\omega}_{robot} = 7.87$ rad/s
- Time for one step: 0.399 sec

As a result of the simulation of frequency adaptation, we obtained

- Frequency: $\hat{\omega}_{robot} = 8.120$ rad/s
- Time for one step: 0.387 sec.

The difference in the frequencies above is roughly 3%. Thus, simple analysis may suggest that the proposed frequency adaptation algorithm achieves the natural frequency of the coupled system through entrainment, i.e., a simple form of resonance tuning.

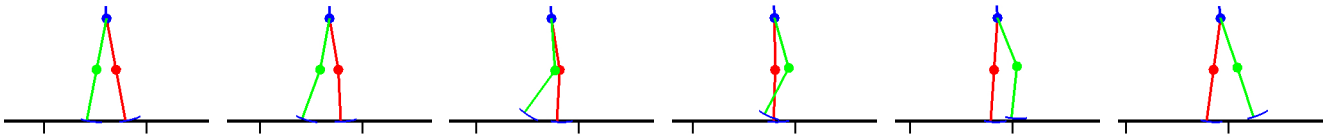

Fig. 11. Snapshots of walking for one step at 15 frames/sec (1 frame ≈ 66msec)

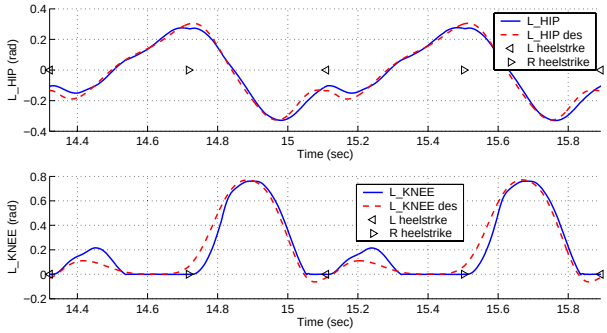

Fig. 9. Joint trajectories for the left leg and heel strike timing of the simulation for two period (4 steps) of walking.

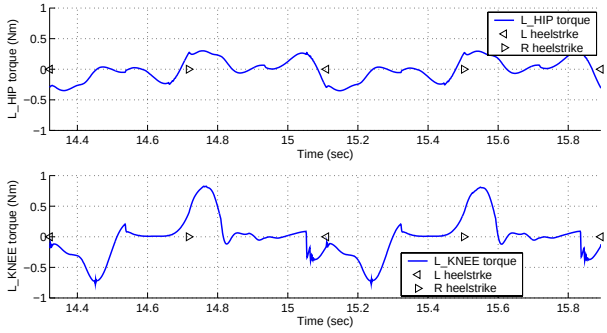

Fig. 10. Torque command to the left hip and knee joints for two period (4 steps) of walking.

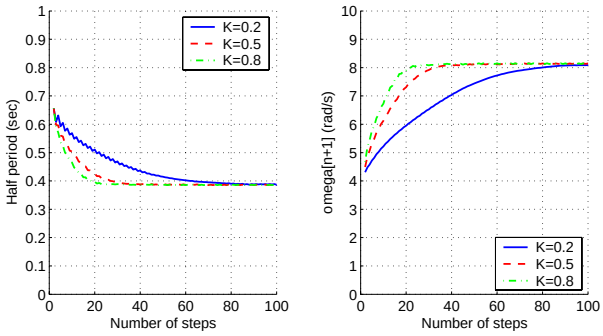

Fig. 12. Frequency adaptation of walking via entrainment.

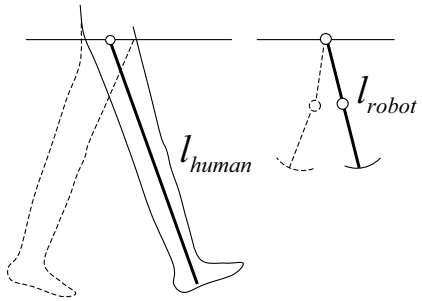

Fig. 13. A simplified pendulum model of the leg with different link length

V. Summary

In this paper, we proposed a method for learning biped locomotion from human demonstration and its frequency adaptation using the dynamical movement primitives. In the dynamical movement primitives, kinematic movement plans are described in a set of nonlinear differential equations with well-defined attractor dynamics, and demonstrated trajectories are learned using locally weighted regression. Specifically, we use rhythmic dynamical movement primitives as a CPG, and introduced a frequency adaptation algorithm through interactions among the CPG, mechanical system and environment. Numerical simulations illustrate the effectiveness of the proposed control algorithm: within a few seconds of walking, the simulation discovered an energy efficient walking frequency, roughly at the natural frequency of the combined robot-oscillator-environment system.

Future work will address intra- and interlimb coordintaion by introducing coupling among oscillators, and recovery from external perturbations. We also consider experimental implementation of the proposed algorithm on our biped robot, and collection of human's walking data under various behavioral conditions. In the long run, we are hopeful that this approach may provide insight into a theoretically sound design principle of biped locomotion control to achieve human-like natural walking.

VI. REFERENCES

[1] Dempster, W. T. and Gaughran, G. R. L., "Properties of body segments based on size and weight," *American Journal of Anatomy*, vol. 120, pp. 33–54, 1965.

[2] Ehara, Y. and Yamamoto, S., *Introduction to Body-Dynamics—Analysis of Gait and Gait Initiation*, Ishiyaku Publishers, 2002, in Japanese.

[3] Fukuoka, Y., Kimura, H., and Cohen, A. H., "Adaptive dynamic walking of a quadruped robot on irregular terrain based on biological concepts," *International Journal of Robotics Research*, vol. 22, no. 3–4, pp. 187–202, 2003.

[4] Hase, K. and Yamazaki, N., "Computational evolution of human bipedal walking by a neuro-musculoskeletal model," *Artificial Life and Robotics*, vol. 3, pp. 133–138, 1999.

[5] Hirai, K., Hirose, M., Haikawa, Y., and Takenaka, T., "The development of honda humanoid robot," In *IEEE International Conference on Robotics and Automation*, pages 1321–1326, 1998.

[6] Ijspeert, A., Nakanishi, J., and Schaal, S., "Movement imitation with nonlinear dynamical systems in humanoid robots," In *IEEE International Conference on Robotics and Automation (ICRA2002)*, pages 1398–1403, 2002.

[7] Ijspeert, A., Nakanishi, J., and Schaal, S., "Learning attractor landscapes for learning motor primitives," In Becker, S., Thrun, S., and Obermayer, K., editors, *Advances in Neural Information Processing Systems 15*. MIT-Press, 2003.

[8] Kagami, S., Kanehiro, F., Tamiya, Y., Inaba, M., and Inoue, H., *AutoBalancer: An Online Dynamic Balance Compensation Scheme for Humanoid Robots*, A K Peters, Ltd., 2001.

[9] Kagami, S., Kitagawa, T., Nishiwaki, K., Sugihara, T., Inaba, M., and Inoue, H., "A fast dynamically equilibrated walking trajectory generation method of humanoid robot," *Autonomouns Robots*, vol. 12, pp. 71–82, 2002.

[10] Kawato, M., "Transient and steady state phase response curves of limit cycle oscillators," *Journal of Mathematical Biology*, vol. 12, pp. 13–30, 1981.

[11] Kotosaka, S. and Schaal, S., "Synchronized robot drumming by neural oscillator," In *Proceedings of the International Symposium on Adaptive Motion of Animals and Machines*, 2000.

[12] Matsuoka, K., "Sustained oscillatons generated by mutually inhibiting neurons with adaptation," *Biological Cybernetics*, vol. 52, pp. 367–376, 1985.

[13] Miyakoshi, S., Yamakita, M., and Furuta, K., "Juggling control using neural oscillators," In *Proceedings of the IEEE/RSJ International Conference on Intelligent Robots and Systems*, pages 1186–1193, 1994.

[14] Morimoto, J., Zeglin, G., and Atkeson, C. G., "Minimax differential dynamic programming: Application to a biped walking robot," In *Proceedings of the IEEE/RSJ International Conference on Intelligent Robots and Systems*, 2003, to appear.

[15] Schaal, S. and Atkeson, C. G., "Constructive incremental learning from only local information," *Neural Computation*, vol. 10, no. 8, pp. 2047–2084, 1998.

[16] Schaal, S., "Is imitation learning the route to humanoid robots?," *Trends in Cognitive Sciences*, vol. 3, no. 6, pp. 233–242, 1999.

[17] Schaal, S., Ijspeert, A., and Billard, A., "Computational approaches to motor learning by imitation," *Philosophical Transaction of the Royal Society of London: Series B, Biological Sciences*, vol. 358, no. 1431, pp. 537–547, 2003.

[18] Strogatz, S. H., *Nonlinear dynamics and chaos: with applications to physics*, Addison-Wesley, 1994.

[19] Taga, G., "Nonlinear dynamics of the human motor control - real-time and anticipatory adaptation of locomotion and development of movements," In *Proceedings of the International Symposium on Adaptive Motion of Animals and Machines*, 2000.

[20] Takanishi, A., Tochizawa, M., Karaki, H., and Kato, I., "Dynamic biped walking stabilized with optimal trunk and waist motion," In *Proceedings of the IEEE/RSJ International Workshop on Intelligent Robots and Systems*, pages 561–566, 1989.

[21] Vukobratović, M., Borovac, B., Surla, D., and Stokić, D., *Biped Locomotion—Dynamics, Stability, Control and Application*, Springer-Verlag, 1990.

[22] Williamson, M. M., "Neural control of rhythmic arm movements," *Neural Networks*, vol. 11, pp. 1379–1394, 1998.

[23] Yamaguchi, J., Takanishi, A., and Kato, I., "Development of a biped walking robot compensating for three-axis moment by trunk motion," In *Proceedings of the IEEE/RSJ International Conference on Intelligent Robots and Systems*, pages 187–192, 1993.